

Electronic Supplementary Material

Temporal and Spatial Temperature Measurement in Insulator-based Dielectrophoretic Devices

Asuka Nakano, Jinghui Luo, Alexandra Ros*

Department of Chemistry and Biochemistry, Arizona State University, Tempe AZ, USA

This supplementary information provides a detailed description of experimental protocols for mitochondria iDEP experiments as well as temperature calibration for method A and B. Additionally, a detailed description of numerical simulations and mathematical formulations are shown. A comparison of temperature measurement and simulations with associate errors is also provided.

Mitochondria iDEP Experiments

After assembly, the microfluidic channels were immediately filled with Buffer A (1 mM F108, 10 mM HEPES, pH adjusted to 7.2~7.4 with KOH) by capillarity and the chip was placed in a humid environment overnight. Then buffer A was removed by vacuum suction, and the channels were washed with Buffer B (10 $\mu\text{g}/\text{mL}$ RhB, 25 mg/mL CHAPS and 250 mM sucrose dissolved in Buffer A) three times and refilled by adding Buffer B to the outlet reservoirs. The conductivity of buffer B is $\sim 300 \mu\text{S}/\text{cm}$. A potential of 3000V was applied for a 1cm long channel for the iDEP experiments using mitochondria.

Temperature Calibration

For the in-channel temperature measurement experiment (method A), fluorescent intensities at various temperatures were measured within a 1 cm diameter chamber for temperature calibration. A Ni-Cr alloy wire (Omega, CT, USA) was embedded inside of the PDMS surrounding the chamber to control the temperature by resistance heating. A solution containing 10 $\mu\text{g}/\text{mL}$ RhB dissolved in pH 8 phosphate buffer with a conductivity of 100 $\mu\text{S}/\text{cm}$ was freshly prepared and filtered through a 0.22 μm syringe filter prior to use. The PDMS chamber containing 1 mL of this buffer was heated by supplying current through the resistive wire. The temperature change was monitored using a K-type thermocouple probe (Omega, CT, USA) in specific increments. For each increment fluorescence intensity was recorded after a constant temperature was reached.

For the method employing the RhB saturated PDMS thin film (method B), the resistive heating wire was directly embedded onto the RhB doped PDMS thin film to control the PDMS surface temperature. The K-type thermocouple probe was attached onto the PDMS to assess the surface temperature.

The resultant calibration curve is shown in Figure S1. Square markers and triangular markers show the sets of data points obtained from method A and B, respectively. The resultant calibration curve is shown with corresponding polynomial fits for method A (blue) and B (red) in comparison with the previously reported calibration curves by Ross et al.¹ (dashed blue line, method A) and Samy et al.² (dashed red line, method B). Method A is in excellent agreement with Ross et al. Note that the difference of the method B calibration curves between ours and the

result by Samy et al. might be attributed to the difference of PDMS film thickness used for the measurements.

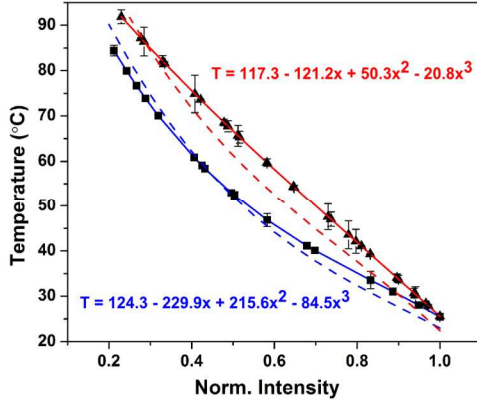


Figure S1. Normalized fluorescence intensity plotted as a function of temperature to calibrate the temperature dependent fluorescence of RhB. Both sets of data obtained from method A (■) and B (▲) are fitted with a third polynomial as indicated in the graph in comparison with the previously reported calibration curves by Ross et al.¹ and Sam et al.².

Numerical Simulations

To elucidate the Joule heating effect in the iDEP device, a numerical model was developed using commercial simulation software *Comsol Multiphysics* (version 4.4, MA, USA). We considered both the fluid in the channel and the solid phase surrounding the channel in the numerical model and solved for the electric current, flow field, and temperature field in 3D. Figure 1 depicts the schematic diagram of the entire geometry used for simulation and its dimensions. First, the electric field distribution was simulated by applying the same potentials used in experiments for each buffer conductivity (100 $\mu\text{S}/\text{cm}$ and 1 mS/cm). All other channel walls were defined as electrically insulating.

We assume a buffer of pH 8 at which negatively charged glass walls create bulk electroosmotic flow (EOF) in cathodic direction. To simulate this flow field, the incompressible Navier-Stokes equation was solved along with the continuity equation. We applied the electroosmotic mobility (μ_{EO}) as a boundary condition to the PDMS walls employing μ_{EO} of $1.5 \times 10^{-8} \text{ m}^2/\text{V s}$ for PDMS channels coated with F108 prior to temperature measurements.³

This Joule heating induced temperature field is governed by the energy equation expressed as:⁴

$$\rho c_p \left(\frac{\partial T}{\partial t} + \mathbf{u}_B \nabla T \right) = k_1 \nabla^2 T + \lambda(T) E^2 \quad (1)$$

where c_p and k_1 denote the specific heat and thermal conductivity of the buffer, respectively, and they are assumed to be independent of temperature. \mathbf{u}_B is the bulk flow velocity, T is the temperature, \mathbf{E} is the electric field, and $\lambda(T)$ is the temperature dependent buffer conductivity. The last term represents the heat generated by Joule heating.

In addition, the heat transfer through the solid is expressed with the following equation:⁴

$$\rho_s c_{ps} \left(\frac{\partial T}{\partial t} \right) = k_s \nabla^2 T + Q \quad (2)$$

where ρ_s , c_{ps} , and k_s denote the density, specific heat, and thermal conductivity of the solid, respectively. Note that our iDEP device is fabricated with the combination of PDMS and glass whose thermal properties differ significantly. Therefore, different values of thermal properties were assigned for the top and side PDMS walls ($k_s = 0.18$ W/m·K, $c_{ps} = 1100$ J/kg·K, $\rho_s = 1030$ kg/m³) and the bottom glass wall ($k_s = 1.4$ W/m·K, $c_{ps} = 835$ J/kg·K, $\rho_s = 2225$ kg/m³). We assume isothermal boundary conditions for the inlet and outlet reservoirs due to the negligible temperature rise at the reservoirs having the large volume. For the outside surface of the channel, the natural convection heat transfer with surrounding air was assumed as boundary conditions, and a heat transfer coefficient (h) of 20 W/m² K was employed.⁵ Upon performing the numerical modeling, the buffer viscosity, buffer electrical conductivity, and the buffer permittivity were treated as temperature dependent, expressed in the following:⁶

$$\mu(T) = 2.761 \times 10^{-6} \exp(1713/T) \quad (3)$$

$$\lambda(T) = \lambda_0 \{1 + 0.02(T - T_0)\} \quad (4)$$

$$\varepsilon(T) = 305.7 \exp(-T/219) \quad (5)$$

where λ_0 is the electrical conductivity of the buffer at room temperature.

We tested both steady-state and time-dependent temperature changes numerically. In the case of the steady-state simulation, all three physics were coupled by taking into account the aforementioned temperature dependent parameters in a 3D device. However, for time-dependent simulation, we solved only the electric current and temperature field with only accounting for the temperature dependency of the electrical conductivity. The electroosmotic velocity was entered in the *Heat transfer in solids* module as a bulk fluid flow velocity as indicated in equation (1). We chose this approach for the 3D time-dependent simulation due to the lack of computation capability and confirmed that the resultant temperature distribution was not affected by employing the simplified methodology.

Comparison of Temperature Measurement and Simulations

Table S1 presents temperature measured experimentally as well as numerically simulated temperature with various buffer conductivities (300 $\mu\text{S}/\text{cm}$, 100 $\mu\text{S}/\text{cm}$, and 1 mS/cm) and applied potentials ranging from 100 V to 3000 V for a 1 cm long channel. Associated experimental errors were calculated as standard deviations of 6 locations within each image from 3 different measurements. Simulation errors were associated with standard deviations of the maximum temperature obtained in the high temperature regions (i.e. between the tips of the triangular posts) from 3 consecutive rows.

Table S1. Comparison of experimentally measured temperature and simulations

Buffer Conductivity	Applied external electric field (V/cm)	Saturation temperature in-channel ($^{\circ}\text{C}$)		Saturation temperature on film ($^{\circ}\text{C}$)	
		Experiment	Simulation	Experiment	Simulation
300 $\mu\text{S}/\text{cm}$ (Buffer B)	3000	34 ± 1	-	-	-
100 $\mu\text{S}/\text{cm}$ (Phosphate buffer)	100	25.0 ± 0.3	25.0 ± 0.1	26.0 ± 0.3	25 ± 0.03
	1000	25.6 ± 0.2	25.3 ± 0.1	25.9 ± 0.1	25 ± 0.1
	3000	28.9 ± 0.1	28.3 ± 0.2	26.4 ± 0.2	26 ± 0.2
1 mS/cm (Phosphate buffer)	100	26.8 ± 0.4	25.0 ± 0.1	25.4 ± 0.2	25 ± 0.1
	1000	29.6 ± 0.2	28.9 ± 0.5	27.0 ± 0.1	27 ± 0.1
	3000	68 ± 2	90.0 ± 2.2	50 ± 1	44 ± 1

References

- (1) Ross, D.; Gaitan, M.; Locascio, L. E. *Anal. Chem.* **2001**, *73*, 4117–4123.
- (2) Samy, R.; Glawdel, T.; Ren, C. L. *Anal. Chem.* **2008**, *80*, 369–375.
- (3) Hellmich, W.; Regtmeier, J.; Duong, T. T.; Ros, R.; Anselmetti, D.; Ros, A. *Langmuir* **2005**, *21*, 7551–7557.
- (4) Bergman, T. L.; Lavine, A. S.; Incropera, F. P.; DeWitt, D. P. *Fundamentals of Heat and Mass Transfer*; 7th ed.; John Wiley & Sons: New York, 2011.
- (5) Bergman, T. L.; Lavine, A. S.; Incropera, F. P.; DeWitt, D. P. *Introduction to Heat Transfer*; 6th ed.; John Wiley & Sons: New York, 2011.
- (6) Haynes, W. M. *CRC Handbook of Chemistry and Physics*; 93rd ed.; CRC Press: Boca Raton, 2012.